# Combining Spectral and Texture Data in the Segmentation of Remotely Sensed Images

**Soren Ryherd and Curtis Woodcock**

## Abstract

*Image segmentation is a method of defining discrete objects or classes of objects in images. Addition of a spatial attribute, i.e., image texture, improves the segmentation process in most areas where there are differences in texture between classes in the image. Such areas include sparsely vegetated areas and highly textured human-generated areas, such as the urban-suburban interface. A simple adaptive-window texture program creates a texture channel useful in image segmentation. The segmentation algorithm is a multi-pass, pair-wise, region-growing algorithm. The test sites include a simulated conifer forest, a natural vegetation area, and a mixed-use suburban area. The simulated image is especially useful because polygon boundaries are unambiguous. Both the weighting of textural data relative to the spectral data, and the effects of the degree of segmentation, are explored. The use of texture improves segmentations for most areas. It is apparent that the addition of texture, at worst, has no influence on the accuracy of the segmentation, and can improve the accuracy in areas where the features of interest exhibit differences in local variance. Results indicate that, for most uses, segmentation schemes should include both a minimum and maximum region size to insure the greatest accuracy.*

## Introduction

Image segmentation is the process of dividing digital images into spatially cohesive units, or "regions." These regions represent discrete objects or areas in the image. Segmented images are useful in many ways, primarily by providing the basic units used in maps when individual pixels in the image are too small to use for this purpose. Also, segmented images can be easier to interpret, by highlighting specific objects in the image. However, automating image segmentation has proven difficult. The human mind segments images unconsciously as it integrates the data perceived through the eyes. To get a computer to effectively partition images has proven to be a complicated task.

A problem arises in segmenting images when the pixels which comprise an individual object in an image are not spectrally homogeneous. Photointerpreters have long known that other clues, aside from spectral brightness, help them to analyze an image. In addition, the texture, shape, orientation, site, and association have been shown to help analysts interpret an image. While it is difficult to quantify many of these aspects of image analysis used by the human mind, some of the above can be measured in ways that are useful in computer-assisted analysis. The research presented here evaluates quantitatively the contribution of texture to image segmentation. In particular, the intent is to evaluate the relative contribution of texture as a function of the characteristics of the image being segmented and to show how to scale the contribution of texture in segmentation.

There are many reasons for segmenting an image into discrete regions. One goal of remote sensing scientists is to map surface phenomena, and often the pixel size in the image is smaller than the desired map units. For example, at the scale of 1:24,000, the minimum size of a usable map unit mightbe on the order of 3 hectares. This minimum size is equal to 33 TM pixels (30-m spatial resolution) or 75 SPOT pixels (20-m spatial resolution). Image segmentation provides a logical transition from the units of pixels to larger units in maps. Another reason for segmenting an image into regions is that subsequent processing steps may require per-region, rather than per-pixel, input. It may be beneficial to assume that each pixel is one of many observations derived from a single object, rather than an independent observation. In fact, many methods and models now require multi-pixel input, particularly where intra-region statistics need to be calculated. A good example is the the use of the Li-Strahler forest canopy reflectance model for mapping forest structure (Woodcock *et al.*, 1990).

### Image Segmentation

Image segmentation is the term given to techniques which partition an image into multi-pixel regions. Haralick and Shapiro (1985), in their survey of image segmentation techniques, separated them into six types: measurement-space-guided spatial clustering, single-linkage region growing, spatial clustering, hybrid-linkage region growing, centroid-linkage region growing, and split-and-merge methods.

Measurement-space-guided clustering involves separating images based on histogram peaks to define classes in the image. Variations on this approach have been attempted by Chow and Kaneko (1972), Weszka *et al.* (1974), Panda and Rosenfeld (1978), Goldberg and Shlien (1978), Ohta *et al.* (1980), and Kohler (1981). As Haralick and Shapiro (1985) point out, this type of segmentation is most likely to avoid errors through poor region merges; however, it does not produce spatially contiguous regions, and some salt-and-pepper effect can occur. At times, post-classification filtering of images has been used to create regions in an image (Kan *et al.*, 1975; Goldberg and Goodenough, 1978; Itten and Fasler, 1979; Thomas, 1980; Logan and Woodcock, 1982; Goldberg *et al.*, 1984). Ton *et al.* (1991) attempted to improve upon this approach through a hierarchical class-based approach which utilized knowledge of the surface features being segmented. Nagao and Matsuyama (1979) developed a limited pre-classification segmentation in their attempt at spatially

Boston University Center for Remote Sensing and Department of Geography, 685 Commonwealth Avenue, Boston, MA 02215.

Photogrammetric Engineering & Remote Sensing, Vol. 62, No. 2, February 1996, pp. 181–194.

0099-1112/96/6202-181$3.00/0

confined smoothing. Spectrally similar adjoining pixels were replaced with mean gray-level values in an attempt to simplify, or smooth, the resulting image. In effect, they were creating regions based on a limited single-band distance of spectral values. This approach was later expanded upon in more complex algorithms.

Single-linkage algorithms involving individual pixel linkages to create regions were developed by Bryant (1979) and Asano and Yokoya (1981); however, the ease of merging inappropriate regions is too great with this form of algorithm. Hybrid single-linkage algorithms attempt to avoid this problem through using a neighborhood characteristic instead of single pixel value. Levine and Leemet (1976) used a shared nearest-neighbor parameter for example, while Reed and Wechsler (1990) surveyed several filter-based approaches for the segmentation of texture images for pattern recognition applications. Others (Haralick, 1984; Haddon and Boyce, 1990; Pavlidis and Liow, 1990) have explored using edge detection techniques for image segmentation.

Landgrebe (1980) combined spatial and spectral information in his ECHO classifier, a combined segmentation and classification algorithm. ECHO attempted to incorporate spatial relationships into a classification scheme. Problems occurring with single-linkage region-growing algorithms can be avoided in centroid-based algorithms. In centroid-based algorithms, the region means are re-computed as regions are merged, thereby forming a more "realistic" basis for further merges. Kauth *et al.* (1977) developed BLOB for reducing noise in the results of classifications of agricultural fields. Although not extensively tested, BLOB did qualitatively improve classification results and the ability to easily outline training areas for use in classifications. A multi-pass approach was developed by Latty (1984) in which edge pixels were first identified based on spectral contrast with adjoining pixels. Goodenough *et al.* (1984) also used edge detection techniques to augment their segmentation of SAR images. Their segmentation algorithm was a graph-theoretic approach first developed by Narendra and Goldberg (1980). Haralick and Kelly (1969) suggested at an early date the use of a combination of measurement space and spatial clustering to determine where clustering should begin. In effect, "seed" locations were determined by histogram peaks in feature space.

Woodcock *et al.* (1983) used Haralick's (1980) sloped-facet model to segment rugged forest landscapes where the criterion for segmentation was based on the slope and aspect of the site. Ioannidis and Kazakos (1985) used a combination of Gaussian Densities and Markov fields to segment a highly textured image. Unfortunately, it is not apparent whether their approach was tested on actual satellite imagery or how well their approach worked. Other approaches in the past (Brill, 1989) have used only the spectral data without taking into account any spatial attributes of the image or objects in the image.

### Texture

Texture can be thought of as the spatial patterns in an image. Textures have been described as smooth, fine, coarse, lumpy, stippled, mottled, and rippled in photogrammetric applications (Ambrosia and Whiteford, 1983). Cross and Jain (1983) discussed attributes of texture in terms of coarseness, contrast, directionality, line-likeness, regularity, and roughness, and attempted to reproduce different textures through the use of a Markov random field model. Their model was successful in creating texture patterns similar to certain types of images.

Most studies to date have sought ways to define texture so as to model natural texture features or to be used in a classification (Mitchell *et al.*, 1976; Khashyap and Khotanzad, 1986; Barber and LeDrew, 1991) or segmentation (Dougherty and Pelz, 1989; Harlow *et al.*, 1986; Reed and Wechsler, 1990; Bouman and Liu, 1991). These approaches at defining texture have included the use of Fourier transforms (Stromberg and Farr, 1986), fractals (Mandelbrot, 1977), random mosaic models (Ahuja and Rosenfeld, 1981; Modestino *et al.*, 1981), mathematical morphology (a binary sieving operation which results in a gray-level texture image (Dougherty and Pelz, 1989)), syntactic methods, and linear models (from Cross and Jain, 1983). Most of these approaches have been in the field of pattern recognition and have not been applied to the analysis of remotely sensed data.

Texture has not always been considered an aid in image analysis. High variance in portions of images make classification difficult when treated in a per-pixel fashion. Cushnie (1987) went so far as to suggest removing textural information entirely through the use of smoothing algorithms in order to improve classification results. The approach here, however, will be to use these spatial data as an information source instead of trying to remove them.

The development of texture as useful spatial information has followed several courses. Texture can be thought of as the spatial pattern of gray levels in an image. The measure used to describe this pattern can take different forms. One method is to pass a filter over the image and use the variance of the pixels covered by the filter as the value of the pixel in the texture image (Jensen, 1979; Agbu and Nizeyimana, 1991; Briggs and Nellis, 1991). This is not the only way to measure texture, however, and there have been other statistics used, as well as differences in the methods described above.

Woodcock and Ryherd (1989) found that using the above local variance texturing technique in an adaptive windowing procedure resulted in an improved image for certain applications. The adaptive window preserved the boundaries between areas of low and high texture (in this case, local variance), while not enhancing or widening the edges, which is one of the side effects of traditional moving-window texture images.

Several investigators have used gray-level co-occurrence (GLC) matrices inbuilding texture images (Harlow *et al.*, 1986; Barber and LeDrew, 1991). The GLC matrix, a matrix of second-order probabilities, has been used to identify periodicity and structure within object texture through a variety of texture statistics. Other statistics computed from co-occurrence matrices, such as entropy, angular second momentum, and inverse difference moment, have also been used (Haralick *et al.*, 1973; Peddle and Franklin, 1991).

## Methods

The approach used to test the effects of using texture in image segmentation involved developing a series of test images for which "ground truth" was available to serve as a reference. Segmentations of images using different combinations of bands and weightings for texture could then be evaluated relative to this "ground truth" standard. For this study, three test images were used: a simulated forest image at TM resolution, a TM image of an area of natural vegetation in central Massachusetts, and a SPOT image in New Jersey of mixed urban and suburban land uses. The test images were selected to provide a variety of landscapes to determine the effect of adding texture under differing environmental conditions, spatial resolutions, and spectral resolutions. The descriptions of these areas and the reference datasets used are included in the discussion of the results of the segmentations for these areas.

In order to test the use of texture in segmentation an adaptive-window variance-based texture image was used. This approach is described in Woodcock and Ryherd (1989), where the digital number (DN) of a pixel in the texture image is the local variance in an adaptively placed 3 by 3 window. A 3 by 3 window was chosen as the most likely to cross spatial resolutions with the least areal effects based on the tem-

plate size. The location of the adaptively located window used to calculate local variance is the window with the lowest local variance of all windows that include the pixel. Thus, in our case of a 3 by 3 window, nine windows are tested. The intent is to calculate texture from the object or region to which a pixel belongs and avoid the edge enhancement associated with the calculation of texture from windows centered on the pixel in question. (An example of a texture image derived using this adaptive-window approach is shown in Figure 8.)

The segmentation algorithm used in all the tests presented in this paper is a multiple-pass region-growing approach designed by Woodcock and Harward (1992), which is based on the Spatially Constrained Clustering algorithm originally developed by Tilton (1983). This algorithm is a centroid-linkage region-growing segmentation algorithm which builds spatially homogeneous regions based on Euclidean distances in n-dimensional space. The algorithm uses a multiple-pass approach with limitations on how many merges are allowed in a single pass. Any given region is allowed only one merge per pass, and only with that region's reciprocally nearest neighbor in n-dimensional feature space. To add an additional check against "rash" merges, a parameter of the program limits the percentage of regions that can be merged in a single pass. For this study, this parameter was set at ten percent for all segmentations.

In the tests of the effect of texture on image segmentation, two variables were varied. The first was the level of segmentation, or how far the segmentation procedure is allowed to continue. If the image is not segmented enough, then the resulting regions are too small to be meaningful. If segmentation is allowed to proceed too far, then many objects in the image are merged into the same region, and the regions are excessively heterogeneous. The optimal answer is a segmentation where the procedure is allowed to progress as far as possible until the regions are too large to accurately represent the landscape features. In this study, the between-band Euclidean distance was used to control the level of segmentation as a user-specified tolerance.

In addition to the use of tolerance levels to control the degree of segmentation, an approach based on using minimum region sizes was used. The use of size criteria to control the segmentation was added because this approach to segmentation produces results more useful for mapping purposes than the tolerance-based segmentations. The reason is that the tolerance-based segmentations tend to produce results that include many individual pixels that remain as regions, and also several very large regions. These kinds of results pose problems for mapping purposes where minimum polygon (or region) sizes are an issue.

The second variable tested is the level of importance, or weighting, of the texture data in the segmentation. Weighting of texture was done by scaling the DN values of the texture image to different ranges. Because the segmentation algorithm works by merging pixels with the least between-band distance, the level of scaling represents the importance or relative weight of each band. It was anticipated that, for most images, scaling the texture too low would provide less than optimal results while, when scaled too high, texture would overwhelm the spectral information and reduce the accuracy of the segmentation. The optimal scaling of the texture data also depends on the type of image being segmented and the amount of local variance in the image.

Measuring the accuracy or quality of a segmentation is difficult, and a new method was devised for this study. The regions resulting from each segmentation were assigned to classes based on the reference "ground truth" image. A simple plurality rule was applied to pixels within the region boundaries to give each region a class label. Once each region had been classified, the resulting image was compared to the reference image, and the accuracy was tabulated. In this scheme, errors occur only when a region crosses a boundary on the reference image. Because of the nature of the accuracy assessment, accuracy drops as the degree of segmentation increases. The reason is that in an un-segmented image each pixel can unambiguously be assigned to a value in the reference image and accuracy will be 100 percent. However, as the level of segmentation increases, errors begin to occur as individual regions cross boundaries in the reference map. The better the segmentation maintains the boundaries as defined in the reference image, the higher the overall accuracy of the segmentation. How long the accuracy remains high as the degree of segmentation increases is a measure of the quality of the segmentation. A poor segmentation that does not capture the characteristics of the landscape will drop in accuracy very quickly as the degree of segmentation is increased. Also note that, once the size of the regions becomes larger than the size of the polygons in the reference image, accuracy has to fall.

This method of measuring accuracy was used to ensure separation of effects associated with segmentation and the subsequent classification of the regions. Because the algorithm is growing regions, then as smaller regions are absorbed, individual class accuracies may fluctuate at another class's expense. These fluctuations are related not only to how well the class boundaries are being preserved, but also to the polygon shapes and sizes, and the degree of fragmentation in the class. So, while overall accuracy can be helpful in understanding the results of a segmentation, individual class accuracies are not helpful.

In order to compare data across segmentations and test sites, it was necessary to normalize the variable that measures the degree of segmentation in an image. This normalization is simply accomplished by a ratio of the number of regions produced by a segmentation to the number of pixels in the image (called the R/P ratio). Using this method, an unsegmented image has a value of 1.0, while an image with an average region size of ten pixels has an R/P value of 0.1. All results presented graph accuracy as a function of the R/P ratio.

## Test Images and Results

### Simulated Forest Image

A simulated forest image was created in order to test the results from a segmentation where the forest-stand boundaries are distinct and unambiguous. The use of predetermined stand boundaries allows for absolute "truth" in evaluating the results of the segmentations, which avoids the bias encountered in manual delineation of polygons and in class definitions. The image was simulated to exhibit the values in a Kauth-Thomas greenness image (Crist and Kauth, 1986) for a western conifer forest based on measurements made in a variety of Sierra Nevada conifer forest stands. The images of forest stands were simulated using the Li-Strahler canopy reflectance model (Li and Strahler, 1985). Forest images were simulated for combinations of three sizes for trees and two densities of crown coverage, resulting in six classes of forest stands. Trees are simulated as randomly located cones on a contrasting background. The trees are illuminated from the east (or the left side of the page) at a solar zenith angle of 30 degrees. In the resulting images of these simulated forests, three different tones are distinguishable: a bright background, dark shadows, and an intermediate tone for illuminated tree crowns. These initial images (Figures 1a to 1f) were simulated at a spatial resolution of 1 metre to preserve the detail of the random location of trees. However, to test the use of texture in image segmentation, these 1-metre images were averaged to 30 metres to simulate the spatial resolution of

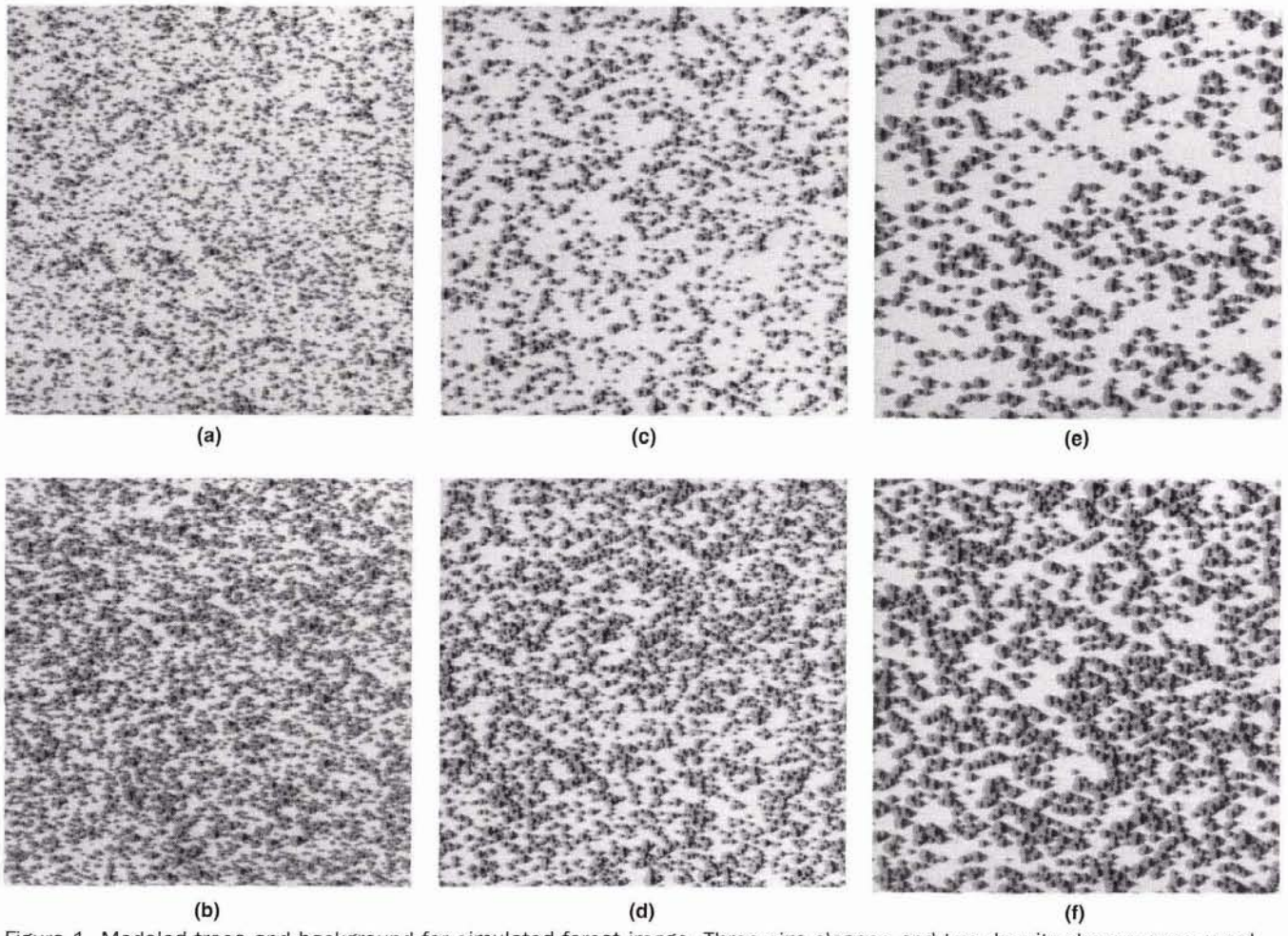


Figure 1. Modeled trees and background for simulated forest image. Three size classes and two density classes were used. (a) Small trees, low density. (b) Small trees, high density. (c) Medium trees, low density. (d) Medium trees, high density. (e) Large trees, low density. (f) Large trees, high density.

Landsat TM images. These six images were then used to fill irregularly shaped polygons which were drawn by hand. Plate 1 shows the hand-delineated stand boundaries with their related size and density class labels, while Figure 2 shows the completed simulated forest image. Table 1 lists the statistics for the six tree classes in the simulated image. It is apparent how increasing tree size increases local variance (texture), while cover chiefly affects the mean spectral response. Given the simulation parameters, the three kinds of sparse and three kinds of dense stands are not spectrally separable. The question involved in segmentation then becomes whether or not the use of texture is sufficient to differentiate stands that have almost identical mean reflectance.

Test segmentations for the simulated image were run with a range of tolerances from 2 to 34, where a tolerance of 2 results in very little segmentation and 34 is highly oversegmented. It was anticipated that the results of segmentations based on a combination of texture and spectral data for the simulated image would result in segmentation accuracies higher than those possible through segmenting either image on its own. This result was anticipated because the spectral differences are dependent upon the density of trees while the differences in the texture channel relate to the tree size classes (Table 1). The results shown in Figure 3 for the tolerance-based segmentations do not support this assumption. The results from segmentations based only on the texture

TABLE 1. IMAGE SIMULATION DATA

| Stand Type (size, cover) | Simulated Forest Images (1-metre) | | | | Simulated TM Pixels | | | |
|---|---|---|---|---|---|---|---|---|
| | percent cover | height mean | height variance | number trees | greenness mean | greenness variance | greenness tex. mean | greenness tex. var. |
| small, sparse | 29.05 | 10.0 | 120.1 | 5247 | 112.0 | 74.0 | 12.9 | 8.4 |
| medium, sparse | 28.48 | 17.5 | 370.3 | 1715 | 111.3 | 169.0 | 9.9 | 7.1 |
| large, sparse | 28.15 | 25.0 | 755.8 | 861 | 110.4 | 357.2 | 6.6 | 4.8 |
| small, dense | 50.15 | 10.0 | 120.1 | 9078 | 80.9 | 60.8 | 11.6 | 12.8 |
| medium, dense | 49.01 | 17.5 | 370.3 | 3430 | 79.1 | 171.0 | 9.8 | 6.6 |
| large, dense | 49.20 | 25.0 | 755.8 | 1723 | 77.5 | 278.9 | 6.2 | 3.1 |

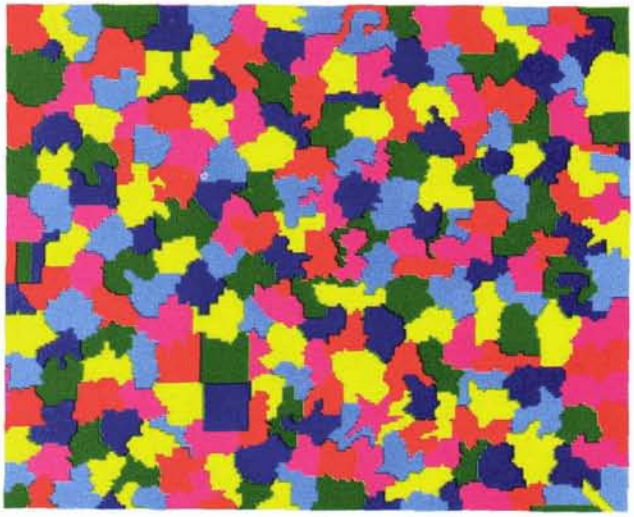

Plate 1. Polygon boundaries for simulated forest reference image. Polygons were hand delineated to be filled with size/density combinations of modeled trees.

| Sparse | Dense |
|---|---|
| Blue – Small Trees | Magnenta – Small Trees |
| Navy – Med. Trees | Yellow – Med. Trees |
| Red – Large Trees | Green – Large Trees |

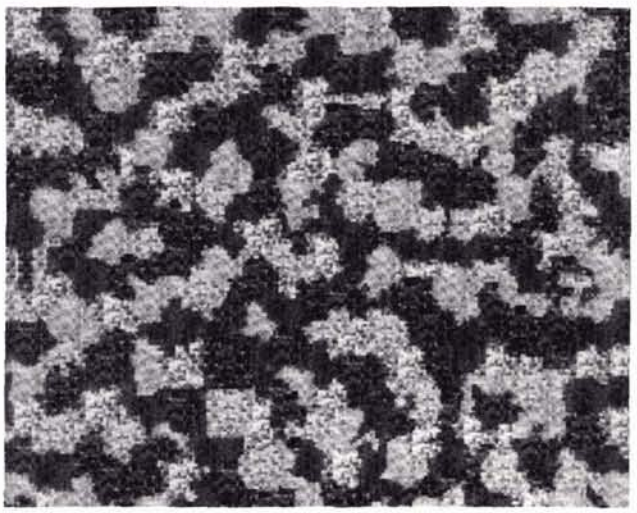

Figure 2. The polygons have been filled with modeled trees and background at six size/density combinations and degraded to TM resolution. The brightness values are typical of a Kauth-Lambert brightness image.

channel are the highest, followed closely by the combined results for spectral and texture data when texutre is heavily weighted. The results become progressively worse as the weighting of the texture is decreased, with the use of only spectral data being the worst. The results from all tests decline dramatically as the degree of segmentation approaches the 0.07 R/P value.

While the texture band alone had the highest accuracy, it is clear that the use of texture in conjunction with the spectral data greatly improves the classification accuracy for this type of landscape. Also, the relationship between texture weighting and accuracy is clear from the definite pattern of increasing accuracy as the weighting of texture increases. It was subsequently found that, in segmentations of actual western conifer forests, a combination of spectral and texture bands was qualitatively better than using either texture or spectral bands alone in the segmentation (Ryherd and Woodcock, 1990).

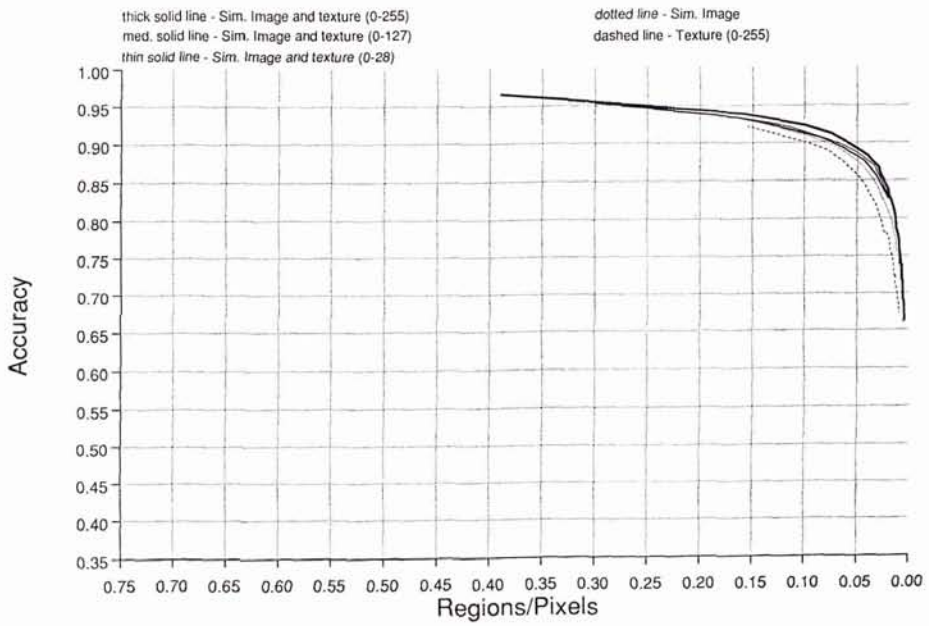


Figure 3. Simulated Image Segmentation Results. Segmentation was run using the simulated forest image and a texture channel. Results using tolerances from 2 to 34 are ratioed to standardize the results and plotted.

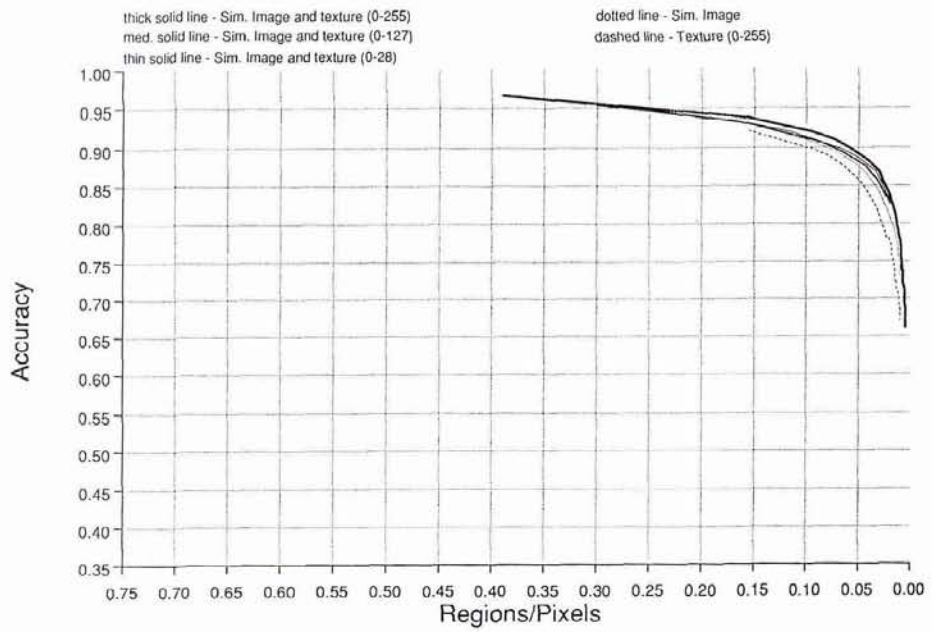


Figure 4. Simulated Image Minimum-Size Segmentation Results. Segmentation was run on the simulated image and texture using minimum-size criteria ranging from 2 pixels to 35 pixels. Results were ratioed to standardize the results and plotted.

The use of a minimum size criterion resulted in quite different accuracy curves. It was anticipated that forcing even-sized stands would increase overall accuracy due to the even-sized nature of the stands in the reference image. The resulting classification accuracies (Figure 4) support this assumptionas all band combinations are higher than the tolerance-based segmentations for equivalent levels of segmentation (R/P values). In addition, accuracies remain high until almost the 0.025-R/P level, and then exhibit a dramatic fall beyond that point as regions begin to exceed the size of stands in the reference image. These accuracy results match our original expectations, with the texture image alone having the lowest overall accuracy, followed by the spectral data, with the combined spectral and texture data having the highest accuracy curves.

A comparison of threshold-based segmentation versus the use of a minimum-size criterion can be seen in Figures 5 and 6. In these figures, the value in each pixel in each region is the mean of the pixels for that region in the simulated greenness image. Figure 5 is a segmented image where the input was the simulated image (greenness band) and the texture band (stretched 0 to 255). This image falls along the central portion of the accuracy curve and has an R/P value of 0.14. It represents what could be considered an "optimal" segmentation in that it is neither over-segmented or under-segmented. However, there are a number of remnant small regions of one or two pixels in areas of high spatial variance. Figure 6 is a segmentation using the same input bands, but forcing merges using the minimum size criterion rather than tolerance. It is selected for comparison because it has a similar overall classification accuracy. The resulting image is clearer, because the noise caused by the very small regions has been removed. This image has an R/P value of 0.03, showing that, while the degree of accuracy is similar (Figures 5 and 6 have accuracies of 0.85 and 0.87, respectively), this image contains far fewer regions. The meaning of this result is that, even with the average region size being larger, overall accuracy is increased because of the lack of a few extremely large regions.

The change in the combinations of bands producing the best results when using size-based segmentation versus tolerance-based segmentation is due to the dramatic increase in the accuracy associated with the use of spectral bands when a minimum size is enforced. The reason for this increased accuracy is that, to achieve the same level of segmentation (R/P value) when no-minimum size is used, some very large regions are created. These large regions have low accuracies, as they cross many boundaries in the reference image. When the minimum size criterion is used, regions don't grow in an unwieldy fashion. Figure 7 illustrates the size distribution of

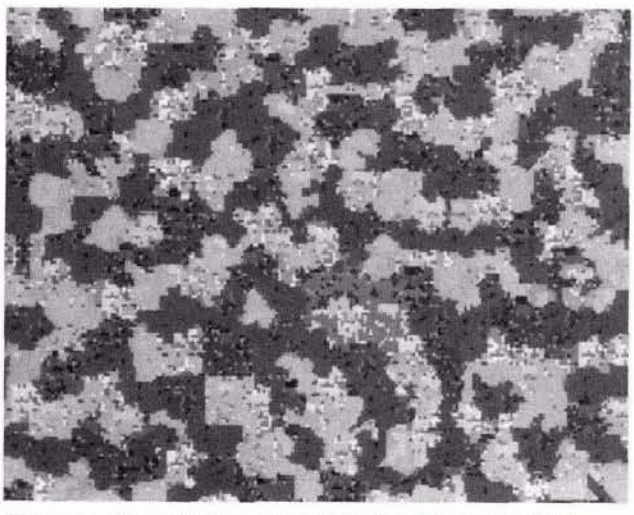

Figure 5. Simulated Image and Texture Segmentation — No Minimum Size. Each pixel in a region has the value of the mean of all pixels for that region from the original simulated forest image. No minimum region size was invoked.

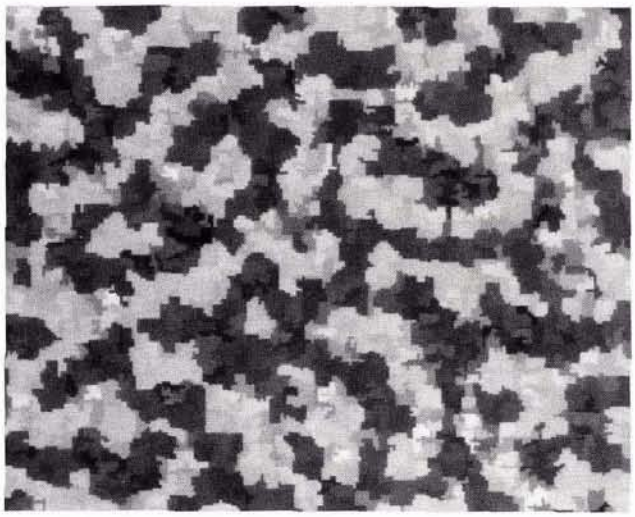

Figure 6. Simulated Image and Texture Segmentation — With Minimum Size. Again, each pixel in a region has the value of the mean of all pixels for that region from the original simulated forest image. A minimum size of 18 pixels per region has been invoked, thus reducing the speckled nature of the segmentation.

regions for both the minimum size and tolerance-based tests. It can be seen that the tolerance-based segmentations have many small regions, but they are not causing the lower accuracy levels, because the measure of accuracy being used here tends to favor small regions. The lower accuracies are being caused by the few very large regions which cross the boundaries in the reference image. When segmented with only the minimum size criteria, the number of these large regions is reduced.

Another factor that may influence the finding that texture alone is more useful for the threshold-based results as opposed to the minimum size segmentations is the nature of the texture image. The texture image is created using an adaptive window where the window location for each pixel is determined by finding the location with the lowest local variance. This causes "blocks" in the image, or areas with the same or very similar texture values (Figure 8). This cubic nature in the resulting image greatly reduces high frequency variability compared to the amount found in most spectral images. In essence, the texture algorithm functions like a low-pass filter. This filtering reduces interpixel variability within the blocks and tends to promote rapid growth or regions inside these blocks. This growth of many moderate sized regions in the segmentation process is desirable, and is enhanced in the threshold-based approach when these texture images are used.

#### Leominster TM Image

Thematic Mapper (TM) imagery of a rural area in New England was used as an example of an area of primarily natural vegetation with closed-canopy forests (Plate 2). Aerial photographs for the same area were interpreted into land-cover classes. A minimum region size equivalent to six TM pixels was maintained in the air-photo interpretation. Surface cover classes were specifically chosen to reflect potential classes of interest to a user, and *not* limited to classes easily separable based on spectral values. These land-cover polygons were then transferred to an enlarged hardcopy of the satellite image and manually digitized. The digitized data were converted to raster format and then registered to the TM image (Plate 3). Table 2 lists the cover types and the means and variances in the bands used for segmentation. It was anticipated that the addition of texture to the segmentation of this area would not greatly improve the accuracy of the segmentation. This is chiefly due to the lack of discernible textural differences between the major forest types in this area because of the high density of forest cover.

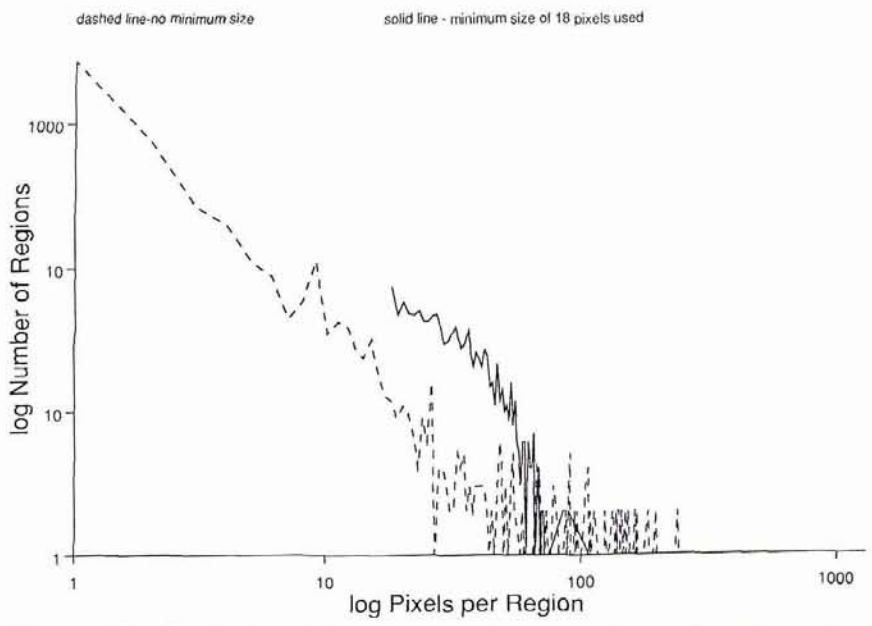


Figure 7. Size Distribution of Segmented Regions. Note the small numbers of large regions in the no-minimum-size segmentation. This is due to the even development of regions when an increasing minimum size is used to control the segmentation.

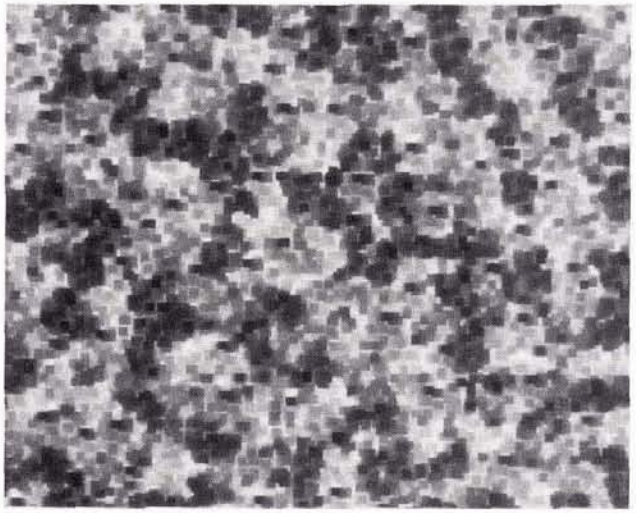

Figure 8. Simulated Forest Image Texture Band. An adaptive-window texture image of the simulated forest image using a 3 by 3 adaptively placed filter. The adaptive-window approach controls the inflation of edge features. The cubic nature of the image is a result of the adaptive-window approach.

The test segmentations for this image were run using combinations of spectral bands 3, 4, and 5, and a texture band created from band 5. The tolerance-based segmentation results indicate that the use of texture alone yields the best segmentations (Figure 9). This result is similar to those observed for the simulated forest image, and again is attributable to the smoothing or filtering effect of the texture algorithm. All other combinations of bands and weights for texture yield very similar results.

When a minimum size criterion is used to control the degree of segmentation, overall accuracies again increase significantly (Figure 10). Also, the results for the segmentations using only texture drop relative to segmentations that include spectral data. There is virtually no difference between the results of the spectral bands with texture or without texture added. It is interesting that in this situation the addition of texture does not degrade the segmentation results. Given the lack of texture differences between classes, it would seem entirely possible that the addition of texture, particularly if it is heavily weighted, could be detrimental. However, our results do not support that idea.

#### Roselle SPOT Image

SPOT multispectral imagery was obtained for an area in New Jersey, near the town of Roselle (Plate 4) to serve as an example of urban and suburban land uses, and as an example using different spatial and spectral resolutions. Again, aerial photographs were used to delineate land-cover polygons, which were then transferred to an enlarged hardcopy print of the SPOT imagery. A minimum polygon size of approximately four SPOT pixels was used. The smaller minimum polygon size was chosen based on the dense mixed-use nature of the landscape. These polygons were digitized and converted to raster format for registration with the SPOT data (Plate 5). Because textural information is often important in discriminating human-made landscapes, this urban-suburban area has been included. Table 3 lists the classes for this test site. It should be noted that some classes exhibit variances either above or below those normally expected for those land-use classes. For example, the waterclass has one of the highest variances, which is unusual because water normally has extremely low variance. The reason for this is the nature of the reference image, which includes many small regions. Often in small classes the "pure" pixels can be outweighed by the more mixed edge pixels. The water class consists of thin segments of the Rahway River, and thus has a high proportion of edge pixels. It is the extremes between the very low infrared reflectance of the water and the high reflectance of the bordering vegetation that creates the high variance in this class. Conversely, single-family residential areas dominate the scene, and while composed of many diverse materials, the overall spectral range is less than the water and vegetation classes. There is also a much lower proportion of edge pixels in the large areas of residential tracts, thus reducing the expected variance. Despite these conditions, most classes do have textural differences, and a look at the texture image (Figure 11) shows that textural boundaries are being preserved.

The suburban fringe of urban areas is difficult to map using per-pixel classifiers because of the highly heterogenous nature of the land-use classes (Jensen and Toll, 1982). Texture has been shown to be useful in these environments in the past, (Conners *et al.*, 1984; Moller-Jensen, 1990) and it is anticipated that a segmentation scheme would improve accuracy. It was also anticipated that the use of texture would further increase the accuracy of classification due to the high level of textural information in this type of area.

Tolerance-based segmentations were run on the Roselle image using the three SPOT spectral bands and a texture band created from spectral band 3 (near-infrared). The results (Figure 12) show that the addition of texture does indeed increase the accuracy of the segmentations. One noticeable result is that the accuracies are much lower for all band combinations compared to the other two sites. This result is due to the fact that the Roselle site is a very complex area comprised of land-use classes that in turn are made up of highly diverse components. The overlapping curves of the mid-range (0 to 128) and full-range (0 to 255) texture weightings indicate that there is some point at which the weighting

TABLE 2. LEOMINSTER SITE STATISTICS

| Class Label | TM Band 3 Mean | TM Band 4 Mean | TM Band 5 Mean | Band 5 Texture Mean | TM Band 3 Variance | TM Band 4 Variance | TM Band 5 Variance | Band 5 Texture Variance | Percent of Image |
|---|---|---|---|---|---|---|---|---|---|
| Mix. For. | 19.42 | 77.88 | 55.76 | 7.29 | 4.40 | 53.18 | 50.65 | 16.57 | 49.03 |
| M.F.-Hardwood | 19.27 | 83.21 | 59.37 | 6.03 | 3.15 | 51.01 | 32.96 | 13.41 | 23.13 |
| M.F.-Conifer | 19.14 | 70.56 | 48.97 | 7.82 | 2.48 | 48.18 | 59.53 | 17.05 | 7.11 |
| Sparse Forest | 19.87 | 76.60 | 59.55 | 7.95 | 3.63 | 67.58 | 64.46 | 16.59 | 5.06 |
| Hardwood | 19.14 | 85.23 | 60.10 | 7.56 | 2.09 | 63.33 | 48.59 | 17.74 | 1.11 |
| Conifer | 19.18 | 76.60 | 59.55 | 5.95 | 1.47 | 51.36 | 47.40 | 7.37 | 1.24 |
| Agriculture | 24.91 | 88.10 | 79.51 | 15.22 | 19.81 | 152.71 | 198.06 | 58.78 | 3.80 |
| Water | 14.34 | 19.90 | 14.32 | 7.77 | 6.47 | 304.30 | 201.31 | 75.74 | 1.72 |
| Wetland | 20.33 | 56.77 | 51.11 | 12.87 | 14.35 | 373.27 | 325.97 | 75.74 | 2.48 |
| Other | 26.00 | 78.35 | 74.54 | 16.58 | 64.07 | 127.68 | 260.67 | 94.93 | 5.31 |

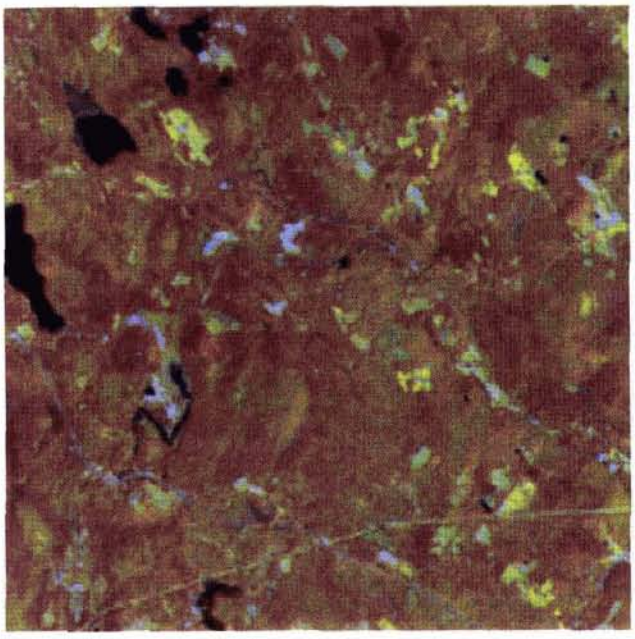

Plate 2. Leominster, Massachusetts TM Image. TM Bands 4, 3, and 2 of a test site near Wachusetts Mountain, Massachusetts.

Plate 3. Leominster, Massachusetts Reference Image. Reference data for the Leominster site derived from digitized photo-interpreted land-use maps.

| | |
|---|---|
| Green | Mixed Forest, Hardwood Dominant |
| Blue | Mixed Forest, Conifer Dominant |
| Red | Mixed Forest, no dominant |
| Yellow | Hardwood Forest |
| Black | Conifer Forest |
| Brown | Sparse Mixed Forest |
| Cyan | Agricultural |
| Light Green | Water |
| Dark Green | Wetlands |
| Magenta | Other |

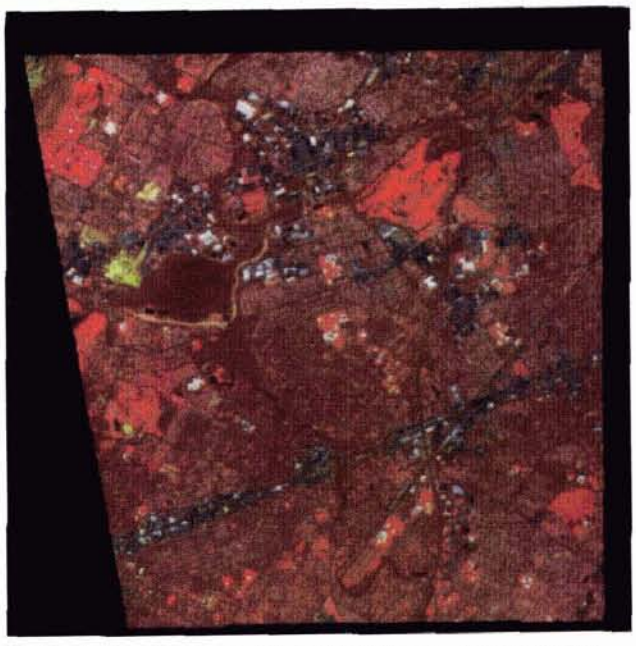

Plate 4. Roselle, New Jersey SPOT Image. SPOT panchromatic bands 3, 2, and 1 for an area in suburban New Jersey, west of New York City.

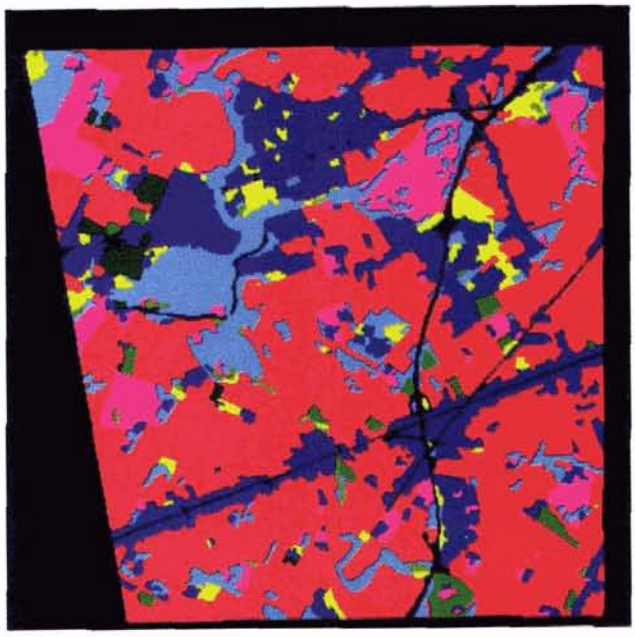

Plate 5. Roselle, New Jersey Reference Image. Reference data for the Roselle site derived from digitized photo-interpreted land-use maps.

| | | | |
|---|---|---|---|
| Red | Single Family Residential | Green | Multi-Family Residential |
| Navy | Commercial | Yellow | Commercial Open Land |
| Cyan | Forest | Magenta | Recreational Open Land |
| Light Green | Water | Dark Green | Agricultural |
| Black | Transportation | | |

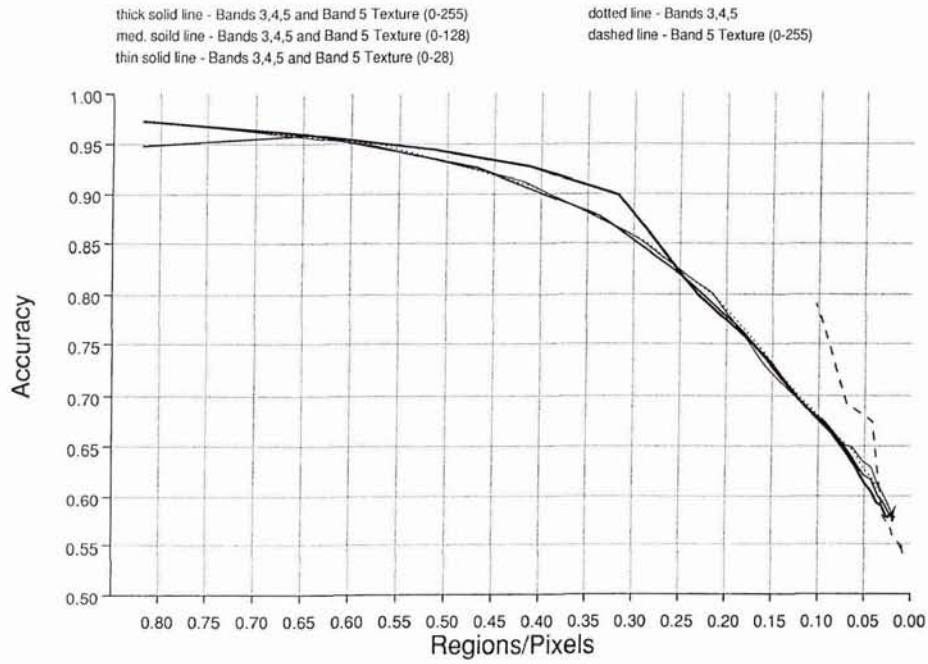


Figure 9. Leominster TM Image Segmentation Results. Segmentation for TM bands 3, 4, and 5 and texture of band 5 were run using tolerance values from 2 to 34. Results were standardized and plotted.

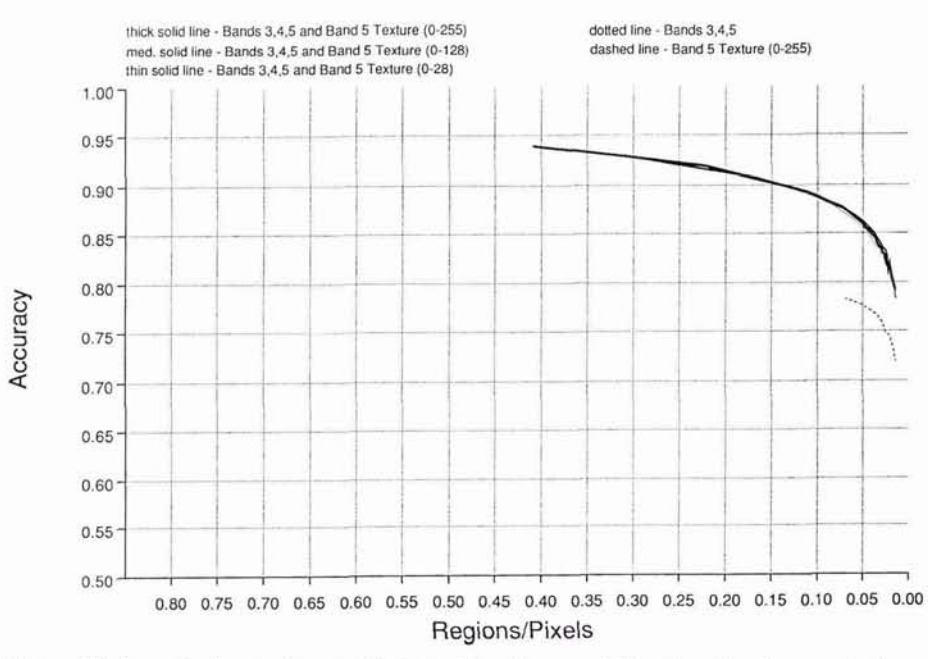


Figure 10. Leominster TM Image Minimum Size Segmentation Results. Segmentation for TM bands 3, 4, 5 and texture of band 5 were run using minimum size limits from 2 to 35 pixels. Results were standardized and plotted.

of texture is playing a crucial part in the segmentation results. This suggests that the texture band may be weighted too strongly in relation to the spectral bands in the 0 to 255 weighting because the accuracy is falling in the later stages of segmentation. This could happen because the blocky nature of the texture image is affecting region boundaries.

When the average region size grows beyond that of the texture filter, there is a slight improvement of the mid-range texture image. Weighting of the texture image at the full range (0 to 255) is causing the texture image to control the segmentation at the high-tolerance end of the accuracy curve. This finding is not surprising, given that the low dynamic

TABLE 3. ROSELLE SITE STATISTICS

| Class Label | SPOT Band 1 Mean | SPOT Band 2 Mean | SPOT Band 3 Mean | Band 3 Texture Mean | SPOT Band 1 Variance | SPOT Band 2 Variance | SPOT Band 3 Variance | Band 3 Texture Variance | Percent of Image |
|---|---|---|---|---|---|---|---|---|---|
| Sing. Fam. Res. | 45.438 | 37.922 | 44.848 | 2.409 | 21.726 | 20.664 | 35.646 | 0.907 | 46.99 |
| Mult. Fam. Res. | 45.955 | 38.620 | 45.763 | 3.068 | 24.236 | 24.767 | 64.493 | 1.565 | 1.39 |
| Commercial | 48.258 | 40.841 | 39.420 | 3.008 | 101.470 | 101.513 | 99.595 | 2.839 | 18.38 |
| Comm. Open Land | 44.718 | 39.049 | 50.041 | 3.340 | 26.486 | 38.744 | 160.501 | 3.413 | 2.81 |
| Recreation | 39.445 | 33.327 | 41.144 | 2.102 | 14.263 | 18.141 | 66.303 | 2.465 | 7.44 |
| Forest | 44.444 | 37.788 | 66.232 | 4.949 | 19.677 | 31.771 | 265.262 | 5.443 | 10.35 |
| Water | 38.466 | 30.684 | 34.121 | 4.610 | 34.881 | 53.242 | 185.804 | 4.993 | 0.49 |
| Agriculture | 49.256 | 47.798 | 52.413 | 2.759 | 34.950 | 92.729 | 63.837 | 1.466 | 0.98 |
| Transportation | 45.144 | 38.428 | 39.322 | 2.852 | 19.888 | 25.627 | 66.304 | 1.856 | 2.52 |

range of the SPOT spectral bands is easily overwhelmed by an additional band, such as texture, having a high dynamic range.

The minimum size segmentation results again show that the use of texture alone compares poorly to the use of spectral channels or spectral channels combined with texture (Figure 13). It surprising to note that, when using the minimum size criterion, there is virtually no difference between using the spectral bands alone or in combination with texture at all weightings. It would be expected that there would be a gradation from having no texture to having the full texture range. The lack of separation by texture weightings indicates that, when a minimum size restriction is invoked, the texture differences that are apparent when no minimum size is used disappear with regards to controlling the segmentation. The use of texture in the segmentation of both this site and the Leominster site resulted in no change between texture weightings when a minimum size is used.

## Discussion

The effects of combining spectral bands and texture in a segmentation scheme have been explored in this research. It was originally thought that texture would provide a measurable, but subtle, improvement in segmentation accuracies when added to the spectral data. What has been shown is that texture, in certain situations, can be a far stronger addition in certain landscapes than had been presupposed. In particular, texture can have strong positive effects when using threshold-based segmentations. This result is due to the nature of the texture image as related to the process of forced merges within a minimum size-controlled segmentation. Because the texture data are derived from spectral differences at the local level where the defining criterion is the least variance, forcing every pixel within a small area to merge results in the same decisions being made in merging at the local level as when the texture data are added as a separate data layer. In effect, the advantages that a texture layer provides are being reproduced by the forcing of a minimum size in the segmentation process. The effect of imposing minimum region sizes is to make the adaptive window texture approach redundant.

It is also apparent from the results that texture is a helpful addition only when the classes in the scene exhibit differences in image texture values. In the images which show differences in texture values, like the simulated forest image and the urban/suburban SPOT image, the addition of texture is helpful. Similarly, where texture values are very similar between classes, such as in the forest classes in the Leominster Thematic Mapper image, the addition of texture does not help. While this finding is not surprising, it does provide a method for deciding whether or not to include texture. One interesting result is that texture generally does not improve segmentations controlled by minimum size criteria.

One final result of interest concerns the lack of negative effects associated with the use of texture. Only when texture was used independently were results worse than for the tests using only the raw spectral bands. Never when texture was combined with the spectral bands were the results degraded. This result bodes well for the use of texture in practical applications of segmentation, as it undermines worries about causing problems by adding texture to segmentations.

An important part of segmenting an image is being able to provide segmented regions of useful size to the user. Using a minimum size criterion has been shown here to improve the accuracy of segmented images, as well as to improve the utility of segmented images, particularly in areas of high spatial variability. One reason for the strength of the results in this regard may be because the test sites used here happen to have a small range of polygon sizes (particularly the simulated forest image). In mapping applications, an optimal approach may be the combination of tolerance-based segmentation and a minimum region size, in order to avoid the salt-and-pepper effect of remnant small regions. In addition, a maximum region size may well be as, or more, important than a minimum region size, because we have seen how a few large regions can grow without control and drastically affect the accuracy of a segmentation.

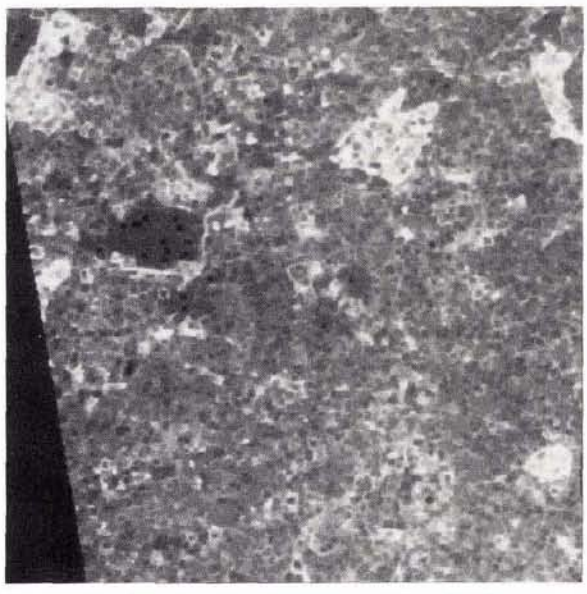

Figure 11. Roselle, New Jersey SPOT Band 3 Texture Image. An adaptive-window texture image of SPOT Band 3 using a 3 by 3 adaptively placed filter.

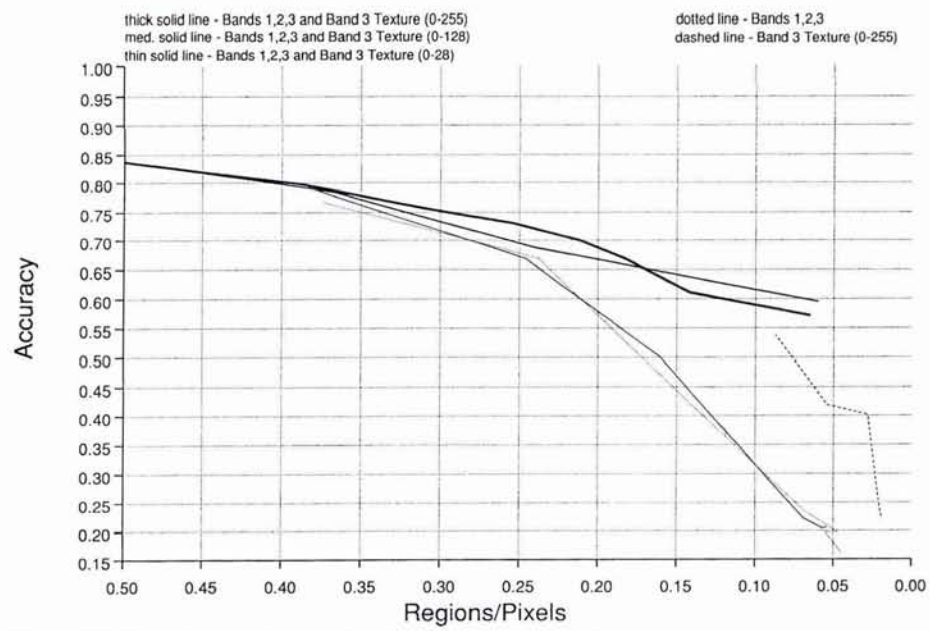


Figure 12. Roselle SPOT Image Segmentation Results. Segmentations were run on SPOT multispectral bands 1,2,3 and texture of band 3 using tolerances running from 2 to 34. Results were standardized and plotted.

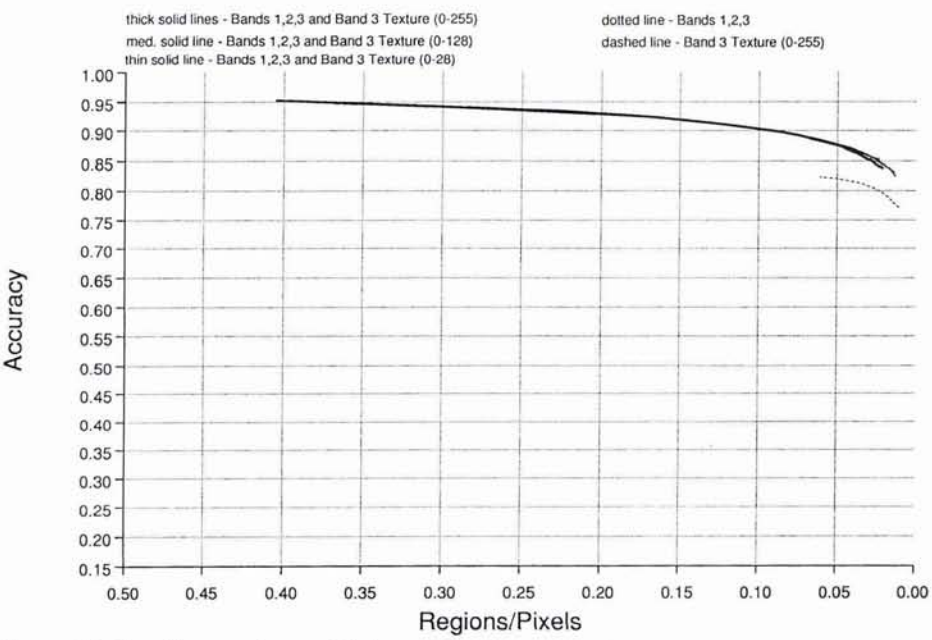


Figure 13. Roselle SPOT Image Minimum Size Segmentation Results. Segmentations were run on SPOT multispectral bands 1, 2, and 3 and texture of band 3 using minimum size limits of 2 to 35 pixels. Results were standardized and plotted. Note that the addition of texture using a minimum size criterion neither improves or detracts from the accuracy.

## Conclusions

From our tests on the effect of using texture data in the segmentation of remotely sensed images, the following can be concluded:

- The addition of texture has stronger benefits in threshold-based segmentations than in minimum-size based segmentations,
- The addition of texture is most beneficial for scenes in which the desired classes exhibit textural differences,
- The combining of texture with spectral data never degraded segmentation accuracies, and
- Segmentations controlled by minimum size criteria produce higher accuracies than threshold-based segmentations.

## Acknowledgments

Funding for this project was provided by Region 5 of the U.S. Forest Service under a joint research agreement between the U.S. Forest Service and the Boston University Center for Remote Sensing. This support is gratefully acknowledged. In addition, Mr. Ryherd was supported by research fellowships under the NASA Graduate Research Program and from the Boston University Center for Remote Sensing (from funds provided by the Keck Foundation). The authors would also like to thank the Boston University Center for Remote Sensing and SPOT Image Corporation for providing test site data for this research.

## References

Agbu, P.A., and E. Nizeyimana, 1991. Comparisons between Spectral Mapping Units Derived from SPOT Image Texture and Field Soil Map Units, *Photogrammetric Engineering & Remote Sensing*, 57(4):397-405.

Ahuja, N., and A. Rosenfeld, 1981. Mosaic Models for Texture, *IEEE Transactions on Pattern Analysis and Machine Intelligence*, PAMI-3(1):1-11.

Ambrosia, V., and G.T. Whiteford, 1983. Aerial Photograph Interpretation in Remote Sensing, *Introduction to Remote Sensing of the Environment* (B.F. Richason, editor), Kendall/Hunt Publishing Company, Dubuque, pp. 57-86.

Asano, T., and N. Yokoya, 1981. Image Segmentation Schema for Low-Level Computer Vision, *Pattern Recognition*, 14:267-273.

Barber, D.G., and E.F. LeDrew, 1991. SAR Sea Ice Discrimination Using Texture Statistics: A Multivariate Approach, *Photogrammetric Engineering & Remote Sensing*, 57(4):385-395.

Bouman, C., and B. Liu, 1991. Multiple Resolution Segmentation of Texture Images, *IEEE Transactions on Pattern Analysis and Machine Intelligence*, PAMI-13(2):99-113.

Bovik, A.C., M. Clark, and W.S. Geiser, 1990. Multichannel Texture Analysis Using Localized Spatial Filters, *IEEE Transactions on Pattern Analysis and Machine Intelligence*, PAMI-12(1):55-73.

Briggs, J.M., and M.D. Nellis, 1991. Seasonal Variation of Heterogeneity in the Tallgrass Prairie: A Quantitative Measure Using Remote Sensing, *Photogrammetric Engineering & Remote Sensing*, 57(4):407-411.

Brill, M.H., 1989. Object-Based Segmentation and Color Recognition in Multispectral Images, submitted to *Proceedings SPIE/SPSE Annual Meeting*, 15-20 January, Paper 1076-11.

Bryant, J., 1979. On the Clustering of Multidimensional Pictorial Data, *Pattern Recognition*, 11:115-125.

Choe, Y., and R.L. Kashyap, 1991. 3-D Shape from a Shaded and Texture Surface Image, *IEEE Transactions on Pattern Analysis and Machine Intelligence*, PAMI-13(9):907-919.

Chow, C.K., and T. Kaneko, 1972. Boundary Detection of Radiographic Images by a Thresholding Method, *Frontiers of Pattern Recognition* (S. Watanabe, editor), Academic Press, New York, pp. 61-82.

Conners, R.W., M. Trivedi, and C. Harlow, 1984. Segmentation of a High-Resolution Urban Scene Using Texture Operators, *Computer Vision, Graphics, and Image Processing*, 25:273-310.

Crist, E.P., and R.J. Kauth, 1986. The Tasseled Cap De-Mystified, *Photogrammetric Engineering & Remote Sensing*, 52(1):81-86.

Cross, G.R., and A.K. Jain, 1983. Markov Random Field Texture Models, *IEEE Transactions on Pattern Analysis and Machine Intelligence*, PAMI-5(1):25-39.

Cushnie, J.L., 1987. The Interactive Effect of Spatial Resolution and Degree of Internal Variability Within Land-Cover Types on Spatial Classification Accuracies, *International Journal of Remote Sensing*, 8(1):15-29.

Dougherty, E.R., and J.B. Pelz, 1989. Textured-Based Segmentation by Morphological Granulometries, *Advanced Printing of Paper Summaries*, Electronic Imaging '89, 2-5 October, Boston, Massachusetts, 1:408-414.

Goldberg, M., and D.G. Goodenough, 1978. Analysis of a Spatial Filter for Landsat Imagery, *Journal of Applied Photographic Engineering*, 4(1):25-27.

Goldberg, M., M.L. Imhoff, and E. Daddio, 1984. Region-Based Modeling Algorithms for Remotely-Sensed Data, *Proceedings Machine Processing of Remotely Sensed Data Symposium*, pp. 205-208.

Goldberg, M., and S. Shlien, 1978. A Clustering Scheme for Multispectral Image, *IEEE Transactions on Systems, Man, and Cybernetics*, SMC-8:86-92.

Goodenough, D.G., B. Guindon, and J.-F. Meunier, 1984. Adaptive Filtering and Image Segmentation for SAR Analysis, *Proceedings, Machine Processing of Remotely Sensed Data Symposium*, pp. 315-324.

Haddon, J.F., and J.F. Boyce, 1990. Image Segmentation by Unifying Region and Boundary Information, *IEEE Transactions on Pattern Analysis and Machine Intelligence*, PAMI-12(10):929-948.

Haralick, R.M., 1980. Edge and Region Analysis for Digital Image Data, *Computer Graphics and Image Processing*, 12:60-73.

———, 1984. Digital Step Edges from Zero Crossing of Second Directional Derivative, *IEEE Treansactions on Pattern Analysis and Machine Intelligence*, PAMI-6:58-68.

Haralick, R.M., and G.L. Kelly, 1969. Pattern Recognition with Measurement Space and Spatial Clustering for Multiple Image, *Proceedings, IEEE*, 57:654-665.

Haralick, R.M., and L.G. Shapiro, 1985. Survey: Image Segmentation Techniques, *Computer Vision, Graphics, and Image Processing*, 29:100-132.

Haralick, R.M., K. Shaunmmugam, and I. Dinstein, 1973. Textural Features for Image Classification, *IEEE Transactions on Systems, Man, and Cybernetics*, SMC-3(6):610-621.

Harlow, C.A., M.M. Trivedi, and R.W. Conners, 1986. Use of Texture Operators in Segmentation, *Optical Engineering*, 25(11):1200-1206.

Ioannidis, A., and D. Kazakos, 1985. Segmentation of Textured Images by a Maximum Likelihood Classifier Using Markov Mesh and Gaussian Joint Density Models, *Proceedings Machine Processing of Remotely Sensed Data Symposium*, p. 343.

Itten, K.I., and F. Fasler, 1979. Thematic Adaptive Spatial Filtering of Landsat Landuse Classification Results, *Proceedings, 13th International Symposium on Remote Sensing of Environment.*

Jensen, J., 1979. Spectral and Textural Features to Classify Elusive Land Cover at the Urban Fringe, *The Professional Geographer*, 4: 400-409.

Kan, E.P., J.K. Lo, and R.L. Smelser, 1975. A New Image Enhancement Algorithm with Applications to Forestry Stand Mapping, *Proceedings, 10th International Symposium on Remote Sensing of Environment*, October, pp. 745-755.

Kashyap, R.L., and A. Khotanzad, 1986. A Model-Based Method for Rotation Invariant Texture Classification, *IEEE Transactions on Pattern Analysis and Machine Intelligence*, PAMI-8(4):472-481.

Kauth, R.J., A.P. Pentland, and G.S. Thomas, 1977. BLOB: An Unsupervised Clustering Approach to Spatial Processing of MSS Imagery, *Proceedings, 11th International Symposium on Remote Sensing of Environment*, 2:1309-1317.

Kohler, R., 1981. A Segmentation System Based on Thresholding, *Computer Graphics and Image Processing*, 15:319-338.

Landgrebe, D.A., 1980. The Development of a Spectral-Spatial Classi-

fier for Earth Observational Data, *Pattern Recognition*, 12: 165-175.

Latty, R.S., 1984. Scene Segmentation through Region Growing, *Proceedings, Machine Processing of Remotely Sensed Data Symposium*, pp. 305-314.

Levine, M.D., and J. Leemet, 1976. A Method for Non-Purposive Picture Segmentation, *Proceedings, Third International Joint Conference on Pattern Recognition.*

Li, X., and A.H. Strahler, 1985. Geometric-Optical Modeling of a Conifer Forest Canopy, *IEEE Transactions on Geoscience and Remote Sensing*, 23(5):705-721.

Lifshitz, L.M., and S.M. Pizer, 1990. A Multiresolution Hierarchical Approach to Image Segmentation Based on Intensity Extrema, *IEEE Transactions on Pattern Analysis and Machine Intelligence*, PAMI-12(6):529-540.

Logan, T.L., and C.E. Woodcock, 1982. User Alternatives in Post-Processing for Raster-to-Vector Conversion, *Technical Papers, Auto Carto V/ISPRS IV*, 22-28 August, Crystal City, Virginia.

Mandelbrot, B.B., 1977. *Fractals — Form, Chance, Dimension*, W.H. Freeman, San Francisco, California.

Mitchell, O.R., C.R. Myers, and W. Boyne, 1976. A Max-Min Measure for Image Texture Analysis, *IEEE Transactions on Computers*, C-25(4):408-414.

Modestino, J.W., R.W. Fries, and A.L. Vickers, 1981. Texture Discrimination Based Upon an Assumed Stochastic Texture Model, *IEEE Transactions on Pattern Analysis and Machine Intelligence*, PAMI-3(5):557-580.

Moller-Jensen, L., 1990. Knowledge-Based Classification of an Urban Area Using Texture and Context Information in Landsat-TM Imagery, *Photogrammetric Engineering & Remote Sensing*, 56(6): 899-904.

Nagao, M., and T. Matsuyama, 1979. Edge Preserving Smoothing, *Computer Graphics and Image Processing*, 9:394-407.

Narendra, P.M., and M. Goldberg, 1980. Image Segmentation with Directed Trees, *IEEE Transactions on Pattern Analysis and Machine Intelligence*, PAMI-2:2.

Ohta, Y., T. Kanade, and T. Sakai, 1980. Color Information for Region Segmentation, *Computer Graphics and Image Processing*, 13:222-241.

Pachowicz, P.W., 1990. Integrating Low-Level Features Computation with Inductive Learning for Texture Recognition, *IEEE Transactions on Pattern Recognition and Artificial Intelligence*, PRAI-4(2):147-166.

Panda, D.P., and A. Rosenfeld, 1978. Image Segmentation by Pixel Classification in (Gray Level, Edge Level) Space, *IEEE Transactions on Comput.*, C-27:875-879.

Pavlidis, T., and Y.-T. Liow, 1990. Integrating Region-Growing and Edge Detection, *IEEE Transactions on Pattern Analysis and Machine Intelligence*, PAMI-12(3):225-233.

Peddle, D.R., and S.E. Franklin, 1991. Image Texture Processing and Data Integration for Surface Pattern Discrimination, *Photogrammetric Engineering & Remote Sensing*, 57(4):413-420.

Reed, T.R., and H. Wechsler, 1990. Segmentation of Textured Images and Gestalt Organization Using Spatial/Spatial-Frequency Representations, *IEEE Transactions on Pattern Analysis and Machine Intelligence*, PAMI-12:1-12.

Ryherd, S.L., and C.E. Woodcock, 1990. The Use of Texture in Image Segmentation for the Definition of Forest Stand Boundaries, *Proceedings, 23rd International Symposium on Remote Sensing of Environment*, Bangkok, Thailand, 18-25 April, 2:1209-1213.

Stromberg, W.D., and T.G. Farr, 1986. A Fourier-Based Textural Feature Extraction Procedure, *IEEE Transactions on Geoscience and Remote Sensing*, GE-24(5):722-732.

Thomas, I.L., 1980. Spatial Postprocessing of Spectrally Classified Landsat Data, *Photogrammetric Engineering & Remote Sensing*, 46(9):1201-1206.

Tilton, J.C., 1983. Multiresolution Spatially Constrained Clustering of Remotely Sensed Data on the Massively Parallel Processor, *Proceedings, Tenth International Symposium on Machine Processing of Remotely Sensed Data*, 12-14 June, Purdue University, W. Lafayette, Indiana, pp. 297-304.

Ton, J., J. Sticklen, and A.K. Jain, 1991. Knowledge-Based Segmentation of Landsat Images, *IEEE Transactions on Geoscience and Remote Sensing*, GRS-29(2):222-232.

Weszka, J.S., R.N. Nagel, and A. Rosenfeld, 1974. A Threshold Selection Technique, *IEEE Transactions on Comput.*, C-23:1322-1326.

Wong, A.K.C., H.C. Shen, and P.W. Wong, 1990. Search-Effective Multi-Class Texture Classification, *IEEE Transactions on Pattern Recognition and Artificial Intelligence*, PRAI-4(4):527-552.

Woodcock, C.E., 1991. GIS Operations Using Image Formats in IPW, preprint of paper presented at *GRASS '91 Users Conference*, 6 March, Berkeley, California.

Woodcock, C.E., and V.J. Harward, 1992. Nested-Hierarchical Scene Models and Image Segmentation, *International Journal of Remote Sensing*, 13(16):3167-3187.

Woodcock, C.E., V. Jakabhazy, S. Macomber, S. Ryherd, A.H. Strahler, and Y. Wu, 1990. Timber Inventory Using Landsat Thematic Mapper Imagery and Canopy Reflectance Models, *Proceedings, 23rd International Symposium on Remote Sensing of Environment*, Bangkok, Thailand, 18-25 April, 2:937-948.

Woodcock, C.E., and S.L. Ryherd, 1989. Generation of Texture Images Using Adaptive Windows, *Technical Papers, ASPRS/ACSM Annual Convention*, 2-7 April, Baltimore, Maryland, 2:11-22.

Woodcock, C.E., A.H. Strahler, and X. Li, 1983. *Database Segmentation and Stratification*, Final Report, NASA/JPL Contract 956213 to University of California, Santa Barbara (Principal Investigator: D.S. Simonett).

(Received 15 April 1993; accepted 20 October 1993; revised 13 October 1994)